

Accepted Manuscript

Title: Silver nanoparticles stabilized by a polyaminocyclodextrin as catalysts for the reduction of nitroaromatic compounds

Author: Marco Russo Francesco Armetta Serena Riela Delia Chillura Martino Paolo Lo Meo Renato Noto



PII: S1381-1169(15)30042-X
DOI: <http://dx.doi.org/doi:10.1016/j.molcata.2015.07.031>
Reference: MOLCAA 9582

To appear in: *Journal of Molecular Catalysis A: Chemical*

Received date: 18-5-2015
Revised date: 16-7-2015
Accepted date: 27-7-2015

Please cite this article as: Marco Russo, Francesco Armetta, Serena Riela, Delia Chillura Martino, Paolo Lo Meo, Renato Noto, Silver nanoparticles stabilized by a polyaminocyclodextrin as catalysts for the reduction of nitroaromatic compounds, *Journal of Molecular Catalysis A: Chemical* <http://dx.doi.org/10.1016/j.molcata.2015.07.031>

This is a PDF file of an unedited manuscript that has been accepted for publication. As a service to our customers we are providing this early version of the manuscript. The manuscript will undergo copyediting, typesetting, and review of the resulting proof before it is published in its final form. Please note that during the production process errors may be discovered which could affect the content, and all legal disclaimers that apply to the journal pertain.

Silver nanoparticles stabilized by a polyaminocyclodextrin as catalysts for the reduction of nitroaromatic compounds

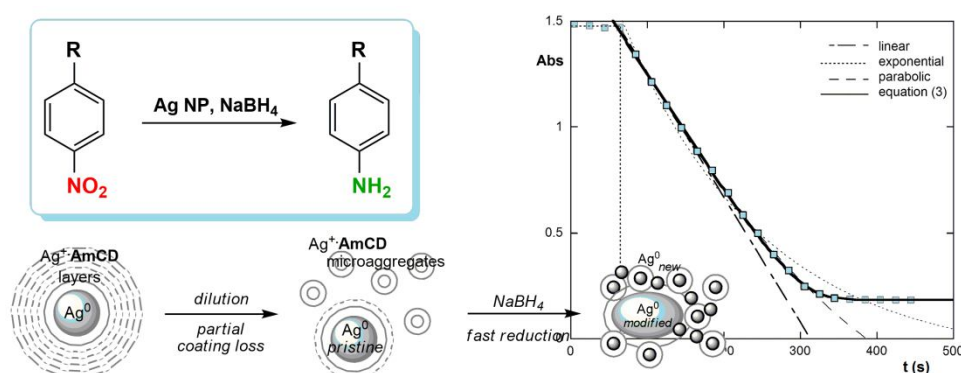
Marco Russo, Francesco Armetta, Serena Riela, Delia Chillura Martino, Paolo Lo Meo,* Renato Noto

Università degli Studi di Palermo, Dip. STEBICEF - V.le delle Scienze, Parco d'Orleans, Ed. 17.

90128 – Palermo (Italy)

e-mail: paolo.lomeo@unipa.it

Graphical abstract



Highlights

- Ag-polyaminocyclodextrin nanocomposites show a layer-organized structure
- These systems were used as catalysts for nitroarene reduction with NaBH₄
- The reduction reaction showed peculiar kinetic features
- Kinetics were rationalized on the by a modified Langmuir-Hinshelwood model
- Results brought us to reconsider some literature mechanistic ideas

Abstract

Silver nanoparticles stabilized by means of *poly*-(6-*N,N*-dimethyl-propylenediamino)-(6-deoxy)- β -cyclodextrin were synthesized, characterized by different techniques (UV-Vis spectroscopy, Dynamic Light Scattering, High Resolution Transmission Electron Microscopy, Fourier-transform IR

Spectroscopy) and used as catalysts for the reduction of various nitrobenzene derivatives with sodium borohydride. The nanocomposites obtained appear to have an organized structure, with a metal core surrounded by a layer-structured coating shell. Kinetic data, rationalized in terms of a modified Langmuir-Hinshelwood model, evidenced a non-linear dependence of the reaction rate on the concentration of the catalyst. This was explained on the grounds of the catalytic activity of differently covered catalyst areas. Careful analysis of kinetic data, in particular the effect of the *para* substituent on the nitroarene structure and the trends of the induction period observed at the beginning of the reaction, provided with interesting insights on the reaction course, and brought us to critically reconsider several mechanistic ideas reported in previous literature.

Keywords

polyaminocyclodextrin

nitroarene reduction

silver nanocomposite

1. Introduction

The reduction of aromatic nitrocompounds is an important synthetic route leading, under the proper reaction conditions, to different nitrogen-containing derivatives [1]. In particular, the reduction to anilines (Scheme 1), which has also a great interest as an industrial process, is generally carried out with strong reducing agents or under harsh conditions. The most common protocols provide the use of LiAlH_4 , transition metals in strongly acidic media (Fe and conc. HCl is a typical industrial method), or catalytic hydrogenation.

Unfortunately, these conditions may be unsuitable whenever particularly delicate functional groups are present in the molecule. Therefore, the availability of milder alternative methods has an undoubted appeal. In this context, the use of NaBH_4 in the presence of noble metal nanoparticles (NPs) has attracted a certain interest [2,3]. The reduction of 4-nitrophenol or 4-nitroaniline (to 4-aminophenol and 1,4-diaminobenzene respectively) has been successfully carried out using NPs stabilized by various capping agents, including biopolymers such as dextran [4,5] or alginate [6-8], and PAMAM- or PPI-type dendrimers [3,9,10]. The latter class of auxiliaries is particularly interesting, because dendrimers provide a strictly defined micro-environment for the formation of the NP and for the actual nitroarene reduction process as well.

Cyclodextrins (**CDs**), both native or chemically modified with suitable donor groups, constitute a class of alternative capping agents for the formation of metal NPs which have been occasionally employed [11,12]. The most known example is probably constituted by the *heptakis*-(6-thiol)-(6-deoxy)- β **CD** [13], which has been successfully used for the synthesis of Au or Ag NPs. Recently, some of us synthesized a new class of polyamino-cyclodextrin products [14], which have been tested as effective auxiliary agents for the preparation of Ag nanoparticles. The **CD** derivatives were obtained by a simple nucleophilic displacement reaction between the *heptakis*-(6-iodo)-(6-deoxy)- β **CD** and various polyamines (Scheme 2).

However, due to the unavoidable occurrence of poly-substitution, the reaction affords mixtures of products bearing a different number of polyamino pendants [15]. As a matter of fact, the same polyamine unit may substitute more than one iodine on the same **CD** scaffold. The obtained materials, which are isolated as partial hydroiodides, have been fully characterized by means of Nuclear Magnetic Resonance, Electrospray Ionization Mass Spectrometry and potentiometric titration. The combined use of these techniques allowed to identify the different constituents of the mixtures, to determine the average number of polyamine pendants (n) and formal HI molecules (x) per **CD** unit, and to calculate the possible protonation or charge status as a function of the pH.

Despite the nitroarene reduction catalyzed by metal NPs has been known for relatively long time, the actual mechanism of catalysis has not been satisfactorily understood, and even the kinetic features of the process are still debated. There is no general agreement about the kinetic order of the reaction, which is usually reported as first order in the nitroarene [3,6,10,12,16-18], but which has been also occasionally described as zeroth order [2,8]. Moreover, the possibility to apply this reaction to further nitroarene derivatives has never been explored in detail. Therefore, a systematic investigation and in general a critical reconsideration of the entire topic seemed interesting. In this context, we reasoned that the use of a cyclodextrin-capped Ag-NP system as the catalyst could be particularly intriguing. Indeed, **CDs** as auxiliary agents may provide both a suitable micro-environment for the formation and the stabilization of the NP, and a sort of receptor site on the catalyst surface, constituted by the **CD** cavity, able to bind and direct the nitroarene substrate.

In the present work we investigated the reduction reaction of various nitroarene derivatives **1-8** (Figure 1) with NaBH₄ in the presence of two Ag-NP catalyst systems, obtained by using the *poly*-(6-*N,N*-dimethyl-propylenediamino)-(6-deoxy)- β CD (**AmCD**, Figure 2) as the capping agent.

The structural and morphological characterization of the Ag-NP systems chosen as catalysts was performed by means of combined UV-Vis spectroscopy, Dynamic Light Scattering (DLS), High Resolution Transmission Electron Microscopy (HR-TEM) and FT-IR spectroscopy. These techniques allowed to get information on the size and polydispersity of the NP suspensions, as well as to investigate the morphology of the NPs. The chosen nitroarene substrates differ for the substituent at the *para* position with respect to the reactant nitro group. They were suitably selected to present significant variations in their molecular properties [19,20]. In particular, we considered the electron-donating effect, the possible charge status and the steric hindrance of the *para* substituent, as well as the intrinsic affinity of the substrate for the CD cavity.

2. Results and discussion

2.1. Synthesis of the NP catalysts

According to previous work [14], **AmCD**-capped Ag-NPs can be obtained by reacting in the dark a solution of the [Ag(NH₃)₂]⁺ complex in the presence of a suitable amount of the auxiliary **AmCD**, with an excess of formaldehyde at 40 °C for 90 minutes. Noticeably, on the grounds of the analytical data reported elsewhere [14], **AmCD** bears on average 5.7 *N,N*-dimethyl-propylenediamino pendants and 4.0 formal HI molecules per CD unit. The formation of the NPs is evident by the appearance of the typical reddish color, due to the characteristic surface plasmon resonance (SPR) absorption band, usually centered between 400 and 450 nm. In a series of preliminary experiments we explored the effect on the NP formation process from changing the concentrations of the reactants and their molar ratio, in particular: *i*) by fixing the [Ag(NH₃)₂]⁺ concentration (1.0 mM) and varying the **AmCD** (0.4~10.0 mN; the normality of the **AmCD** solution is defined according to the average number of donor sites, namely 11.4, per CD unit); *ii*) by fixing

the **AmCD** (2 mN) and varying the $[\text{Ag}(\text{NH}_3)_2]^+$ (0.2~5.0 mM); *iii*) by simultaneously varying both the reactants, while keeping constant their equivalent ratio (2:1 eq/eq, i.e. the same as in the starting $[\text{Ag}(\text{NH}_3)_2]^+$ complex). The obtained systems were preliminarily characterized by UV-vis spectroscopy; the results obtained are summarized in Table 1.

The outcome of the NP formation process strictly depends on the **AmCD**/ $[\text{Ag}(\text{NH}_3)_2]^+$ equivalent ratio used. Nearly no reaction occurred with ratios larger than 4:1. In the other cases the systems showed an absorption band centered at 401 ± 2 nm, the intensity of which (expressed by the relevant molar extinction coefficient, ϵ) regularly increases on decreasing the equivalent ratio. Moreover, the same ratio heavily affects the stability of the system. Samples obtained with a 2:1 ratio are stable for several weeks, if kept in the dark at room temperature. By contrast, systems with a 0.4:1 ratio or prepared with the largest $[\text{Ag}(\text{NH}_3)_2]^+$ concentrations, appear cloudy or turbid and form reddish-brown precipitates within few days (lower ratios were also explored, indeed, but resulted in the quick separation of part of the reduced Ag as the typical "silver mirror"). On the whole, these preliminary findings suggest that the auxiliary **AmCD** protects the silver ion towards its reduction under the conditions used. Data indicate that NP formation is hampered at the highest **AmCD**/ $[\text{Ag}(\text{NH}_3)_2]^+$ ratios, is partial for the ideal 2:1 value, and becomes almost complete at the lowest ratios. Of course, the presence of a minimum amount of **AmCD** is needed in order to ensure the actual formation and stabilization of the NP system. Therefore, it seems reasonable to hypothesize that NPs prepared with a 2:1 ratio are constituted by a metal core, surrounded by a shell of **AmCD** units complexing a certain amount of Ag^+ ions by means of their the amine donor groups. The presence of a significant positive charge on the NP surface ensures the time stability of the system. On the other hand, in systems prepared at low (namely 0.4:1) ratios the NPs formed bear nearly no charge on their surface, and consequently may aggregate or coalesce.

In order to confirm these hypotheses, we thoroughly investigated two particular representative NP systems, which were subsequently used as the catalysts for studying the nitroarene reduction reaction. These systems, indicated hereinafter as Catalysts **I** and **II**, were prepared at a 1 mM $[\text{Ag}(\text{NH}_3)_2]^+$ concentration, and **AmCD** concentrations as large as 0.4 mN (Catalyst **I**) and 2 mN (Catalyst **II**), which correspond to **AmCD**/ Ag^+ mole/mole ratios (ρ) as large as 0.035 and 0.175 respectively. Moreover, as it will be illustrated more in detail in section 2.3, in order to perform the nitroarene reduction reaction Catalysts **I** and **II** are subjected to dilution (up to 1:750 v/v., i.e.

1.33 μM) and subsequent interaction with NaBH_4 . This may cause deep modifications in the structure of the nanocomposite, as it can be evidenced by simple observations. After dilution 1:1 or 1:9 v/v of the preformed Catalyst **II** with water, a significant enlargement and decrease in intensity of the SPR band centered at 401 nm, and the appearance of a new band at 567 nm can be noticed in the normalized UV-vis spectra (Figure 3). The corresponding color change is apparent even at naked eye. The observed behavior might account in principle for either an increase in NP average size, or concomitant changes in the polar character and/or the local refractive index of the coordination shell immediately surrounding the metal core [21]. Furthermore, the residual Ag^+ possibly present at the NP surface (in particular in the case of Catalyst **II**) can be easily reduced to Ag^0 by borohydride ion. As a matter of fact, addition of NaBH_4 to a solution containing $[\text{Ag}(\text{NH}_3)_2]^+$ and **AmCD** (at the

same concentrations as in Catalyst **II**) instantaneously causes the formation of a turbid brown suspension, which precipitates down in few minutes. For these reasons, together with “as-prepared” Catalysts **I** and **II**, we subjected to characterization three further control systems, namely two dilutions 1:1 and 1:9 v/v of Catalyst **II** with water (indicated as **IldilA** and **IldilB** respectively), and a mixture 1:1 v/v between Catalyst **II** and a freshly prepared NaBH_4 48.0 mM solution (indicated as **Iired**).

2.2. Structural and morphological investigation of the NP catalysts

The knowledge of NPs size and morphology is of utmost importance in order to rationalize their activity as catalysts [22]. These information are typically achieved by means of direct methods such as transmission electron microscopy (TEM), as well as by indirect scattering-based methods such as Dynamic Light Scattering (DLS). The latter one affords an evaluation of particle size in suspension, allowing to analyze a more statistically representative sample at the cost of lack in high resolution details about the morphology of nanoparticles. For our purposes, it is worth stressing here that TEM and DLS provide with complementary information about the structural organization of our systems: the former focuses on the metal core alone, whereas the latter looks at the entire nanocomposite, including its coating and hydration shell.

As representative examples, TEM micrographs for Catalysts **I** and for control systems **IldilB** and **Iired** are shown in Figure 4 (further images are provided in the Supporting). The pristine Catalysts **I** and **II** show well defined, quite spherical, individual metal cores with a relatively low polydispersity and scarce tendency to aggregation. Statistical analysis of TEM images indicates unimodal

diameters distributions centered at ca. 27 and 19 nm respectively. Therefore, larger NPs are formed in the presence of a lesser amount of capping agent. Dilution does not seem to have significant effects on the dimensions of the pristine metal cores; however, a fair tendency to aggregation can be noticed, together with the appearance of a new population of small faint objects having an average diameter of ca. 3.6 nm. Considerable modifications are apparent after treatment with NaBH_4 . TEM images show a large tendency to aggregation, together with modification of both the size and the morphology of the pristine metal cores and, most interestingly, the formation of new small sized cores. Statistical analysis of images reveals a completely different diameter distribution, with a maximum frequency centered at ca. 9.7 nm.

Different information are provided by DLS determinations. Data for “as-prepared” systems indicate the presence of smaller aggregates for Catalyst **I** than for Catalyst **II**, with average diameters as large as 86 and 149 nm respectively. Sizes were evaluated by applying the CONTIN method (see Experimental for details; representative DLS curves are reported in Supporting), and again show unimodal distributions. For the control systems **IIdiA** and **IIdiB** average diameters of 149 and 59 nm respectively are found, indicating that significant dilution (namely 1:9 v/v) causes a noticeable decrease of the aggregate size. By contrast, once Catalyst **II** is treated with NaBH_4 , for the system **Iired** the aggregates in suspension grow dramatically in size, with an average value of the diameter of 464 nm, and show high polydispersity. The latter result is in agreement with TEM evidence of NPs aggregation.

It is interesting to notice that, on the grounds of TEM results, metal cores for Catalysts **I** and **II** may be estimated to possess on average $6 \cdot 10^5$ and $2 \cdot 10^5$ silver atoms respectively, and average surface areas as large as 2300 and 1100 nm^2 respectively. On the other hand, simple molecular models suggest that a single **AmCD** unit may cover an area on the NP surface, which can be roughly estimated as comprised between 3 and 7 nm^2 [23]. Keeping into account the actual composition of the systems, in particular the values of the aforementioned **AmCD**/ Ag^+ mole ratios ρ (section 2.1), it can be calculated that only a minor fraction (less than 5%) of the **AmCD** present might actually come in direct contact with, and fully cover, the metal core. It must be also considered that the height of a single **CD** torus is reported to be 0.79 nm [24]; therefore, a single **AmCD** layer cannot be much thicker than 1 nm. Thus, everything considered, the whole of the TEM and DLS results can be explained as follows (Scheme 3).

Pristine NP cores, formed after the slow formaldehyde reduction of silver ions embedded in a sort of $\text{Ag}^+\text{-AmCD}$ macroaggregate, are initially surrounded by a thick layer-structured coating, constituted by shells of **AmCD** units held together by various supramolecular interactions, including the mutual inclusion of the polyamine tails into the **CD** cavities and the complexation of residual Ag^+ ions with the polyamines. This coating offers both a steric and an electrostatic barrier against the aggregation/coalescence of the NPs and, of course, is thicker for Catalyst **II**, prepared with the largest amount of **AmCD**. Dilution of the **catalyst** causes the progressive dissolution of the coating shells (as accounted for by the decreased size estimated by DLS), with formation of small $\text{Ag}^+\text{-AmCD}$ microaggregates (the faint objects observed in **II**d*IB*), which act as seeds for the formation of new small Ag cores after treatment with NaBH_4 . The latter process may cause the deposition of further metal on the pristine cores, modifying their size and shape (as observed in **II**red). The concomitant exhaustive reduction of Ag^+ removes at the same time the electrostatic barrier, causing extensive aggregation.

Further confirmation for the composite nature of our AgNP systems was achieved by means of FT-IR evidence. By subjecting a large amount of Catalyst **I** to centrifugation, a sample of Ag NPs was isolated and its IR spectrum (KBr) was recorded. Noticeably, owing to the strong intrinsic absorption due the nanosized Ag component, the sample disc results fairly opaque to IR radiation. After suitable correction, however, the resulting spectrum shows very intriguing features (Figure 5).

Comparison with the spectrum of free **AmCD**, reveals the presence in the composite of the signals expected for the organic capping agent. More in detail, we observe that the pristine large **AmCD** band at 3310 cm^{-1} , due to superimposition (because of extensive hydrogen bonding) of the -OH and -NH- groups stretching, splits in two bands centered at 3470 and 3136 cm^{-1} respectively. This indicates a neat discrimination between the two different groups, reasonably owing to the occurrence of the N-Ag interactions at the NP surface. The **AmCD** fingerprints at 1153 , 1086 , 1041 (C-O stretching) and 943 cm^{-1} (-OH bending) attributable to the **CD** scaffold, are present in the spectrum of the composite with minor shifts, together with new bands at 998 and 839 cm^{-1} . The latter one, in particular, replaces the corresponding **AmCD** band centered at 756 cm^{-1} which can be attributed to N-H wagging. Therefore, this large shift confirms the occurrence of strong N-Ag

interactions at the primary CD rim. Finally, The spectrum of the composite shows the trivial C-H stretching bands (3000~2800 cm^{-1}), and two strong bands at 1456 and 1385 cm^{-1} due to carbonate ion (superimposed to the expected C-H bending bands of the AmCD at 1466 and 1368 cm^{-1}), the presence of which can be easily explained as due to CO_2 uptake by the quite alkaline NP solution.

2.3. Kinetic study of the nitroarene reduction

In order to study the kinetics of the reduction reaction of nitroarenes **1-8** mediated by Ag-NPs, sample systems were prepared by mixing the proper amounts of stock solutions of the reactants and the catalyst (see Experimental), in such a way to have initial concentrations of the substrate and NaBH_4 as large as 0.1 mM and 4.0 mM respectively, and a catalyst concentration ranging between 1.33 and 83.3 μM . The latter concentration is expressed as the equivalent concentration of silver ion (C_{Ag}) needed to obtain the amount of NPs introduced in the sample. The reducing agent, which is the last component introduced in the system immediately before starting the registration of the kinetic trace, is always used in large excess with respect to the nitroarene substrate. Kinetic experiments were performed at 313 K, following by UV-vis spectrophotometry the disappearance of the absorption band of the substrate, at its λ_{max} value. A typical kinetic trace is shown in Figure 6.

In agreement with literature [2,17,25,26,27], a preliminary induction period is present. Subsequent data points monotonically decrease, till a plateau is almost abruptly reached. In striking contrast with previous literature, the decreasing branch of the kinetic trace cannot be satisfactorily fitted neither as the exponential decay expected for a first order process, nor as a simple straight line accounting for a zeroth-order process. Rather, experimental points appear tentatively adaptable at a first approximation by a parabolic trend. In a preliminary set of control experiments performed with 4-nitroaniline **1**, we fixed the amount of catalyst (50 μM) and suitably varied the borohydride concentration in the range 1.0~8.0 mM. We verified that the initial reaction rate, as expressed by the first order coefficient (c_1) of the fitting parabolic curve, linearly increases with the reducing agent concentration within the range considered (Figure 7, see data in Supporting). According to previous reports [5,23,28], a curvilinear dependence of the initial rate vs. borohydride concentration would have been expected at much larger concentrations (> 10 mM).

The kinetics of NPs catalyzed reactions has been frequently approached by means of the Langmuir-Hinshelwood model [7,18,25,29-31], providing the reversible association of the reactants on different sites of the catalyst surface. This, in particular, explains the curvilinear dependence of the initial reaction rate [5,28], which has been rationalized admitting a fast association pre-equilibrium between the catalyst and the BH_4^- ion, followed by the transfer of a hydride ion onto the NP surface [7,25,32]. However, we preferred to develop a modified version of the model. In particular, we considered the Ag-NP catalyst surface divided in effective area cells **a**, each as large as the average surface covered by a single **AmCD** unit. Then, we hypothesized that the reaction product is formed in a rate-limiting step from a surface-substrate-borohydride ternary complex, deriving through a set of fast pre-equilibria (Scheme 4).

It can be assumed that **a** cells have an actual concentration (C_a) proportional to C_{Ag} according to the relationship $C_a = \sigma C_{Ag}$, where σ is the ratio between the total surface for the NPs generated by one mole of silver ion, and the average surface which can be covered by one mole of **AmCD** units. From Scheme 4 the following differential kinetic expression can be written:

$$v = -\frac{d | ArNO_2 |}{dt} = k | a \cdot BH_4^- \cdot ArNO_2 | = \frac{k K_{BR} C_a | BH_4^- | | ArNO_2 |}{1 + K_B | BH_4^- | + K_R | ArNO_2 | + K_{BR} | BH_4^- | | ArNO_2 |} \quad (1)$$

where K_B , K_R and K_{BR} are the stability constants for the binary (**a**- $ArNO_2$) and (**a**- BH_4^-) complexes and the overall stability constant for the ternary (**a**- BH_4^- - $ArNO_2$) complex respectively; k is the kinetic constant for the rate determining step. Equation (1) can be simplified by considering that the observed linear dependence of the reaction rate on $|BH_4^-|$ implies the algebraic condition: $1 + K_R | ArNO_2 | \gg K_B | BH_4^- | + K_{BR} | BH_4^- | | ArNO_2 |$, then:

$$-\frac{d | ArNO_2 |}{dt} = \frac{k K_{BR} C_a | BH_4^- | | ArNO_2 |}{1 + K_R | ArNO_2 |} = \frac{k K_{BR} \sigma C_{Ag} | BH_4^- | | ArNO_2 |}{1 + K_R | ArNO_2 |} \quad (2)$$

which is equivalent to the expression expected on the grounds of the original Langmuir-Hinshelwood model. It has to be pointed out [31] that an expression such as equation (2) is never approached as such, because it can be reduced to either a first order or a zeroth order expression,

by imposing the conditions $1 \gg K_R |\text{ArNO}_2|$ or $1 \ll K_R |\text{ArNO}_2|$ respectively. Nevertheless, it can be integrated as:

$$t = t_i + (1/k_{obs})(C_0 - |\text{ArNO}_2|) + (1/k_{obs}K_R) \ln(C_0/|\text{ArNO}_2|) \quad (3)$$

where t_i is the length of the induction period, C_0 the starting concentration of the substrate and $k_{obs} = k(K_{BR}/K_R)\sigma C_{Ag} |\text{BH}_4^-|$. The latter condition may be also written as $k_{obs} = kK_{B^*}\sigma C_{Ag} |\text{BH}_4^-|$, where K_{B^*} is the equilibrium constant for the association between the preformed ($\mathbf{a}\text{-ArNO}_2$) binary complex and BH_4^- . Evidence for the occurrence of a strong association between nitroarenes and Ag-NPs, by Raman spectroscopy, has been already reported in literature [16,33]. The integrated equation (3) comprises both a zeroth-order (linear) and a first-order (logarithmic) term in the substrate. So, it can be suitably used to accomplish an excellent fitting the experimental kinetic traces, as shown in Figure 6 [34].

The expression for k_{obs} predicts a linear dependence of the reaction rate on both the concentrations of the reducing agent and the catalyst as well [18, 35]. Surprisingly, however, experimental results showed for k_{obs} a non-linear dependence on C_{Ag} (Figure 8, the complete set of data is collected in the Supporting). In some cases, namely with Catalyst II and anionic substrates **2** (sodium *N*-4-nitrophenyl-glicinate), **3** (sodium *N*-methyl-*N*-4-nitrophenyl-glicinate) and **5** (sodium 4-nitrophenate), we even found non-monotonical trends. No reaction could be observed for substrate **7** (sodium 4-nitrobenzoate) with both catalysts, and for **8** (nitrobenzene) with Catalyst II.

Keeping into account the characterization of the catalysts discussed in Section 2.2, the observed dependence of k_{obs} on C_{Ag} can be explained considering that, under the high dilution condition used, the catalyst should have lost most of its coating. Thus, we can hypothesize that the effective surface cells **a** may be present in the reaction system in three different conditions, namely naked, covered with one **AmCD** unit only, or covered with two (or even more) **AmCD** layers. Of course, differently covered **a** cells are each other in equilibrium and have different catalytic effectiveness. In particular, we can assume that doubly-covered (or even multiply-covered) cells should be catalytically inactive, because the reactants are likely to interact with the outer **AmCD** layer, so they cannot approach the catalytically active NP surface. This has been verified in a set of control experiments performed with 4-nitroaniline **1** and Catalyst I (50 μM). As a matter of fact, by adding

increasing amounts of **AmCD**, we noticed a progressive decrease in the reaction rate, until substantial inhibition was achieved for **AmCD** concentrations larger than 1.0 mM. Therefore, we considered a more complex mechanistic scheme (Scheme 5), keeping also into account the possible host-guest binding equilibrium between the free **AmCD** and the nitroarene substrate. **A similar inverse dependence of the reaction rate on the amount of capping agent has been reported for the reduction of nitrophenol with Au NPs stabilized with natural extracts of *Breyhnia rhamnoides* [16].**

In principle, the reaction rate should depend on the concentrations of the possible active catalyst-substrate-borohydride ternary complexes, according to the expression:

$$\begin{aligned} v &= k_{(0)} | \mathbf{a} \cdot \text{ArNO}_2 \cdot \text{BH}_4^- | + k_{(1)} | (\mathbf{a} \cdot \mathbf{AmCD}) \cdot \text{ArNO}_2 \cdot \text{BH}_4^- | = \\ &= k_{(0)} K_{R(0)} K_{B^*(0)} | \mathbf{a} | | \text{ArNO}_2 | | \text{BH}_4^- | + k_{(1)} K_{(1)} K_{R(1)} K_{B^*(1)} | \mathbf{a} | | \mathbf{AmCD} | | \text{ArNO}_2 | | \text{BH}_4^- | \end{aligned} \quad (4)$$

From Scheme 5, considering the mass balance on the surface cells and the equilibrium conditions, and applying few suitable simplifications, we can obtain the following kinetic equation:

$$\begin{aligned} v &= - \frac{d | \text{ArNO}_2 |}{dt} = k_{(0)} | \mathbf{a} \cdot \text{BH}_4^- \cdot \text{ArNO}_2 | + k_{(1)} | (\mathbf{a} \cdot \mathbf{AmCD}) \cdot \text{BH}_4^- \cdot \text{ArNO}_2 | = \\ &= \frac{[(k_0 K_{R(0)} K_{B^*(0)} + k_{(1)} K_1 K_{R(1)} K_{B^*(1)} | \mathbf{AmCD} |) \cdot \sigma C_{\text{Ag}} | \text{BH}_4^- | | \text{ArNO}_2 |]}{(1 + K_1 | \mathbf{AmCD} | + K_1 K_2 | \mathbf{AmCD} |^2) + (K_{R(0)} + K_1 K_{R(1)} | \mathbf{AmCD} | + K_1 K_2 K_{R(2)} | \mathbf{AmCD} |^2) | \text{ArNO}_2 |} \end{aligned} \quad (5)$$

In equation (5) the concentration of free **AmCD** is accounted. The total amount of **AmCD** in the system (C_{CD}) is bound to C_{Ag} by the relationship: $C_{\text{CD}} = \rho \cdot C_{\text{Ag}}$, where ρ is the **AmCD**/[Ag(NH₃)₂]⁺ mole ratio defined above (Section 2.1). However, at a first approximation it may be assumed $| \mathbf{AmCD} | \approx \rho \cdot C_{\text{Ag}}$, i.e. the concentrations of the various complexes may be considered negligible with respect to free **AmCD** [36]. Then, the following final kinetic expression can be obtained:

$$v = - \frac{d | \text{ArNO}_2 |}{dt} = \frac{(k_0 K_{R(0)} K_{B^*(0)} + k_{(1)} K_1 K_{R(1)} K_{B^*(1)} \rho C_{\text{Ag}}) \sigma C_{\text{Ag}} | \text{BH}_4^- | | \text{ArNO}_2 |}{(1 + K_1 \rho C_{\text{Ag}} + K_1 K_2 \rho^2 C_{\text{Ag}}^2) + (K_{R(0)} + K_1 K_{R(1)} \rho C_{\text{Ag}} + K_1 K_2 K_{R(2)} \rho^2 C_{\text{Ag}}^2) | \text{ArNO}_2 |} \quad (6)$$

Despite its complicated appearance, equation (6) assumes to the same form as equation (2), and can be integrated in the same way to afford the **final** expression:

$$t = t_i + (1/k_{\text{obs}})(C_0 - | \text{ArNO}_2 |) + (1/k_{\text{obs}} K_{\text{app}}) \ln(C_0 / | \text{ArNO}_2 |) \quad (7)$$

where:

$$k_{obs} = C_{Ag} |BH_4^-| \frac{[\sigma k_{(0)} K_{B^*(0)}] + [\sigma k_1 K_1 (K_{R(1)} / K_{R(0)}) K_{B^*(1)}] \rho C_{Ag}}{1 + K_1 (K_{R(1)} / K_{R(0)}) \rho C_{Ag} + K_1 K_2 (K_{R(2)} / K_{R(0)}) \rho^2 C_{Ag}^2} \quad (8)$$

and

$$K_{app} = \frac{K_{R(0)} + K_1 K_{R(1)} \rho C_{Ag} + K_1 K_2 K_{R(2)} \rho^2 C_{Ag}^2}{1 + K_1 \rho C_{Ag} + K_1 K_2 \rho^2 C_{Ag}^2} \quad (9)$$

Equation (8) can be also written as:

$$\frac{k_{obs}}{|BH_4^-|} = \frac{k_{obs,0} C_{Ag} + k_{obs,1} K_{app,1} \rho C_{Ag}^2}{1 + K_{app,1} \rho C_{Ag} + K_{app,2} \rho^2 C_{Ag}^2} \quad (10)$$

where $k_{obs,0} = \sigma k_0 K_{B^*(0)}$, $k_{obs,1} = \sigma k_1 K_{B^*(1)}$, $K_{app,1} = K_1 (K_{R(1)} / K_{R(0)})$ and $K_{app,2} = K_2 (K_{R(2)} / K_{R(1)})$. Noticeably, $k_{obs,0}$ and $k_{obs,1}$ provide a quantitative estimation of the catalytic efficiency of the naked and the singly-covered NP surface respectively. The catalytic efficiency depends, in turn, on the morphological characteristics of the NPs (accounted for by σ), on the ability of the NP-substrate pre-complex to bind the reducing agent (accounted for by $K_{B^*(0)}$ or $K_{B^*(1)}$) and on the intrinsic reactivity of the substrate onto the particular catalyst cell (accounted for by k_0 or k_1); $K_{app,1}$ and $K_{app,2}$ represent the conditional binding constants between the NP surface and the **AmCD** layers in the presence of the different substrates.

Equation (10) can adequately describe the non-monotonical k_{obs} vs. C_{Ag} trends observed with Catalyst **II** and anionic substrates. However, as long as data relevant to Catalyst **I** are considered, the use of equation (10) leads to unreliable $K_{app,2}$ values, characterized by unacceptably large indeterminations. From an algebraic viewpoint, being the term $K_{app,1} K_{app,2} \rho^2 C_{Ag}^2$ negligible with respect to $1 + K_{app,1} \rho C_{Ag}$, a simplified form of equation (10) can be more suitably used:

$$\frac{k_{obs}}{|BH_4^-|} = \frac{k_{obs,0} C_{Ag} + k_{obs,1} K_{app,1} \rho C_{Ag}^2}{1 + K_{app,1} \rho C_{Ag}} \quad (11)$$

The results obtained in analyzing the apparent kinetic constants k_{obs} for substrates **1-8** with either equation (10) or (11) are summarized in Table 2.

We can notice that $k_{obs,0}$ values span over a much larger range for Catalyst **II** than for Catalyst **I**, indicating larger variations in reactivity between the various substrates, and therefore a larger selectivity for the catalyst. Moreover, larger $K_{app,1}$ values are generally observed with Catalyst **I** than with Catalyst **II**. These differences among the two catalysts may be ascribed to the different amount of unreduced Ag^+ ion present on the catalyst, which is likely to interact with the nitroarene substrate before the addition of borohydride. Then, after BH_4^- is introduced to start the title reaction, it also reduces the residual Ag^+ . Thus, the consequent modifications in the morphology of the catalyst may be affected by the possible occurrence of significant Ag^+ -substrate interactions. This seems particularly evident in the case of anionic substrates, for which non-monotonical trends in k_{obs} values vs. C_{Ag} are observed.

Analysis of data reported in Table 2 indicates that the presence of a strong electron-donating substituent at the *para* position with respect to the reacting nitro group, is an important requirement for the reaction to occur. As far as $k_{obs,0}$ values are concerned, nitroanilines **1-4** and nitrophenate **5** appear significantly more reactive than nitroanisole **6** and nitrobenzene **8**, whereas nitrobenzoate **7** is not reactive at all. This result might appear quite surprising, because the reduction reaction should imply either an electron transfer process [16,37] or the nucleophilic attack of a hydride species to the nitro group. The latter type of process is consistent with the hypothesis reported in literature that BH_4^- transfers a hydride ion onto the NP surface [7,25,32]. In both cases the reaction should be unfavorably affected by electron-donating substituents. By contrast, the behavior observed indicates that the mechanistic course of the process provides the interaction of the nitroarene with an electrophilic species, which must be identified with the catalyst surface. Nitroanilines **1-4** give further insights on the role of the *para* substituent group. *N*-substituted derivatives **2-4** do not appear more reactive than parent nitroaniline **1**, despite alkyl substituents on the N atom should enhance the overall electron-donating character of the group. Therefore, the presence of a negative charge on the ancillary chain bound to the N atom (substrates **2** and **3**), or the occurrence of significant steric hindrances (substrate **4**), play an unfavorable role. This probably reflects a more difficult approach of the anionic reducing agent to the nitroarene-catalyst pre-complex, and a lower stability of the reactive ternary complex. The

reactivity of nitrophenate **5** with Catalyst **II** appears exceptionally high. This is probably due to peculiar modifications in the NP surface morphology, occurring as a consequence of particular Ag^+ -substrate interactions, as discussed previously.

On passing to analyze $k_{obs,1}$ values, we can immediately notice that the singly-covered surface cells appear by far less catalytically active than uncovered ones. More in detail, $k_{obs,0}/k_{obs,1}$ ratios range from 4.6 (substrate **4** with Catalyst **II**) up to 97 (substrate **5** with Catalyst **I**). A lesser activity for singly-covered cells is not a trivial finding, because it indicates that inclusion into the receptor-like cavity does not lead the nitroarene to approach more easily the catalytic surface. This, however, is in contrast with the fact that the organic molecule is correctly included with the nitro group directed towards the primary **CD** rim [19,20,38]. By considering data for Catalyst **I**, the lowest $k_{obs,1}$ values are observed for substrates **2** (sodium *N*-(4-nitrophenyl)-glycinate) and **5** (sodium 4-nitrophenate). The former one is known to form a very stiff inclusion complex with native βCD [20], due to the occurrence of multiple hydrogen bonding with the secondary host rim. The same effect likely blocks this substrate quite rigidly within the **AmCD** cavity. By contrast, other substrates unable to undergo multiple hydrogen bonding form more flexible complexes [20], and consequently are able to slip down more easily onto the NP surface after inclusion. It is interesting to notice that even the parent nitrobenzene **8** appears relatively reactive onto the singly-covered catalyst. Finally, the scarce reactivity of **5** may be likely attributed to the occurrence of a strong hydrogen bond interaction of the anionic centre with the secondary host rim, which forces its average position far from the NP surface.

A few considerations are due to the apparent binding constants K_{app} present in equations (7) and (9) and to the conditional binding constants $K_{app,1}$ and $K_{app,2}$ present in equations (8), (10) and (11). K_{app} reflects the actual contribution from the first order term to the overall reaction kinetics. This contribution increases in importance as K_{app} decreases; consequently, larger deviations are observed in the kinetic trace with respect to the ideal linear trend expected for a purely zeroth order process. Unlike a true binding constant, K_{app} depends on the concentration of the catalyst according to equation (9). Observed values usually range between $4 \cdot 10^4$ up to $4 \cdot 10^5 \text{ M}^{-1}$, and frequently show bell-shaped trends as a function of C_{Ag} , with few exceptions. However, these values are affected by very large indeterminations (up to 40 %), so that a detailed analysis would be a pointless exercise. On passing to $K_{app,1}$ and $K_{app,2}$, their values depend on both on the intrinsic affinity of the **AmCD** towards the naked or singly covered NP surface (irrespective of the substrate, as accounted for by K_1 and K_2 respectively), and on the different abilities of the naked, singly- or

doubly-covered cells to bind the nitroarene (as accounted for by the ratios (K_{R1}/K_{R0}) and (K_{R2}/K_{R1})). Therefore, large differences in $K_{app,1}$ or $K_{app,2}$ among different substrates have to reflect similar differences in the latter ratios. For instance, nitrobenzene **8** shows with Catalyst **I** a much smaller $K_{app,1}$ value as compared to the other substrates. This clearly mirrors its much lesser affinity for the host cavity, consequent to the smaller value of its binding constant with native β CD [39] as compared with nitroanilines. The same argumentation can be applied to nitroanisole **6** with Catalyst **II**. However, it should be reminded that $K_{app,1}$ values for Catalyst **II** are influenced by the deep modifications of the catalyst upon introduction of the reducing agent, as discussed previously. The outcome of the possible substrate- Ag^+ interactions on such modifications is not easily predictable. Regarding $K_{app,2}$, its estimation was possible only in few cases, but values appear quite lower as compared to $K_{app,1}$. It is worth stressing that $K_{app,2}$ accounts for the interaction between superimposed layers of **AmCD**, which probably involves the inclusion of the diamine pendants of the outer layer into the cavities of the inner one. Therefore, data suggest that **the latter interaction is significantly less effective.**

Finally, regarding induction times t_i , for each substrate-catalyst combination examined we observed that values increase on decreasing the concentration of the catalyst (data for substrate **1** with Catalyst **I** are shown in Figure 9 as a representative example).

Induction times vary with both the substrate and the catalyst. Nitroanilines **1-4** show smaller values than nitrophenate **5** and nitroanisole **6**, whereas nitrobenzene shows the largest values. At the largest NP concentrations, slightly shorter induction times are observed with catalyst **I**, with the exception of nitrophenate **5**. The occurrence of an induction period has been justified in different ways. It was formerly admitted that the catalytic process can start only after a tiny layer of silver oxide possibly present on the NP surface had been reduced by BH_4^- [2]. It has been alternatively proposed that induction times (viewed as the inverse of a sort of kinetic constant [25]) might be related to the diffusion of the reacting species onto the catalyst surface [17], or to the reconstruction of the NP surface [25]. Our results, however, seem to rule out these interpretations, because they cannot **explain neither the observed dependence on the concentration of the catalyst and on the structure of the substrate as well, nor the fact that induction occurs also with Catalyst **II**, having a significant amount of Ag^+ immediately reduced *in situ* by borohydride.** On the other hand, it is well known that induction is typical for mechanisms involving free-radical species. Therefore, it might be tentatively interpreted as an indication that

the nitroarene substrate undergoes single electron transfer processes leading to short-lived radical species, which are scavenged by the molecular O₂ present in solution [40]. There is literature evidence that induction times for 4-nitrophenol reduction are suppressed by exclusion of O₂ from the reaction system [27]. As a consequence, the target reaction cannot properly start unless all the O₂ has been consumed by reaction with the excess borohydride. The latter process will be catalyzed by NPs and, as a consequence, its duration will depend on the concentration of the catalyst. On the other hand, it can be expected that the NP-substrate interaction will favor this process, with an increasing effect on increasing the electron-donating character of the substrate itself.

3. Conclusions

Polyaminocyclodextrin-capped Ag NPs were synthesized and characterized by combined UV-vis, DLS and TEM techniques. Our systems appear constituted by a metal core surrounded by a layered coating shell, made by the AmCD units held together by supramolecular interactions such as tail-cavity mutual inclusion or complexation of the residual unreduced Ag⁺ ions. This shell offers both a steric and an electrostatic barrier to aggregation, but it is progressively dissolved upon dilution on the system. Then, possible treatment with NaBH₄ causes both a modification of the size and shape of the pristine metal cores and the formation of new small cores.

Two Ag-AmCD NP systems were used as catalysts for the reduction of nitroarene derivatives with sodium borohydride. The reaction shows a peculiar kinetic trend and an unexpected dependence of the apparent kinetic constants k_{obs} on the concentration of the catalyst. On the grounds of a modified Langmuir-Hinselwood model, experimental data were rationalized by means of a complex mechanistic scheme, providing the possibility that the catalyst surface may be present in the reaction system partly naked, and partly covered with one or more AmCD layers. Data show that the reaction course is favorably affected by the presence of electron-donating groups on the substrate, indicating that the NP surface acts as an electrophile towards the nitro group. Nevertheless, the presence of negatively charged or bulky groups on the substrate has a slightly unfavorable outcome, probably due to a more difficult approach of the reducing agent. The AmCD-covered catalyst surface seems less active, because of the intrinsic stability of the substrate-AmCD inclusion complex. In the case of Catalyst II, which contains a significant amount

of unreduced Ag^+ ion, its morphology changes as BH_4^- is introduced into the reaction system. The latter process may be significantly affected by the presence of the substrate. Finally, the trends for the induction period seem to provide evidence for the occurrence of free-radical pathways in the intimate mechanism of reduction of the nitro group.

4. Experimental

4.1. Materials

All commercial (Aldrich, Fluka) reactants and materials were used as purchased, with no further purification. The nitroaniline derivatives **2-4** were prepared according to literature [19,20], by a nucleophilic aromatic displacement reaction between 4-nitrofluorobenzene and the proper amine. The *poly*-(6-*N,N*-dimethyl-propylenediamino)-(6-deoxy)- β CD **AmCD** [14] was synthesized by a nucleophilic displacement reaction between the *heptakis*-(6-iodo)-(6-deoxy)- β CD and a 20-fold excess of 3-(*N,N*-dimethylamino)-1-aminopropane (which functions as the solvent too), at 60 °C for 48 h. Its high-resolution ESI-MS spectrum gave the following signals: 990.4720 ($\text{C}_{77}\text{H}_{154}\text{N}_{14}\text{O}_{28} \cdot 2\text{HI} \cdot 2\text{H}$)⁺⁺, 873.5507 ($\text{C}_{77}\text{H}_{154}\text{N}_{14}\text{O}_{28} \cdot \text{H} \cdot \text{Na}$)⁺⁺, 862.5601 ($\text{C}_{77}\text{H}_{154}\text{N}_{14}\text{O}_{28} \cdot 2\text{H}$)⁺⁺, 820.5090 ($\text{C}_{72}\text{H}_{140}\text{N}_{12}\text{O}_{28} \cdot \text{H}_2\text{O} \cdot 2\text{H}$)⁺⁺, 811.5024 ($\text{C}_{72}\text{H}_{140}\text{N}_{12}\text{O}_{28} \cdot 2\text{H}$)⁺⁺, 778.4575 ($\text{C}_{67}\text{H}_{126}\text{N}_{10}\text{O}_{28} \cdot 2\text{H}_2\text{O} \cdot 2\text{H}$)⁺⁺, 769.4513 ($\text{C}_{67}\text{H}_{126}\text{N}_{10}\text{O}_{28} \cdot \text{H}_2\text{O} \cdot 2\text{H}$)⁺⁺, 760.4447 ($\text{C}_{67}\text{H}_{126}\text{N}_{10}\text{O}_{28} \cdot 2\text{H}$)⁺⁺, 582.7033 ($\text{C}_{77}\text{H}_{154}\text{N}_{14}\text{O}_{28} \cdot 2\text{H} \cdot \text{Na}$)⁺⁺⁺, 575.3765 ($\text{C}_{77}\text{H}_{154}\text{N}_{14}\text{O}_{28} \cdot 3\text{H}$)⁺⁺⁺, 547.3417 ($\text{C}_{72}\text{H}_{140}\text{N}_{12}\text{O}_{28} \cdot \text{H}_2\text{O} \cdot 3\text{H}$)⁺⁺⁺, 541.3379 ($\text{C}_{72}\text{H}_{140}\text{N}_{12}\text{O}_{28} \cdot 3\text{H}$)⁺⁺⁺. All other physical and spectroscopic data (m.p., IR, ¹H NMR, ¹³C NMR) were consistent with literature.

4.2. Instrumentation

ESI-MS mass spectra were recorded in positive mode on an AGILENT Technologies 6540 UHD Accurate Mass Q-TOF LC-MS apparatus (1 kV nozzle voltage, 250 V fragmentor voltage). UV-vis spectra were recorded on a Beckmann DU 800 spectrophotometer, equipped with a Peltier thermostatic apparatus, which was used also to perform the kinetic experiments. FT-IR spectra (2% in KBr) were acquired on a Bruker VERTEX 70 apparatus.

TEM micrographs were acquired using a JEM-2100 (JEOL, Japan) electron microscope operating at 200 kV accelerating voltage. A drop of each suspension was put onto a 3 mm Cu grid "lacey carbon" for analysis and let the solvent to complete evaporation.

DLS measurements have been carried out by using a 90 Plus Particle Size Analyzer (Brookhaven Instrument Corp., Holtsville, NY, USA) equipped with a BI-9000AT Digital Autocorrelator. The source was a He-Ne 632.8 nm laser and the detector was a photomultiplier tube, both mounted on a turntable; measurements were performed at 90°. By using the software supplied by Brookhaven Institute, data were obtained directly as electric field self-correlation function, $G(\tau)$, versus decay time, τ . In order to check data reproducibility and the stability of the suspension, measurements have been repeated in triplicate on different freshly prepared samples. Electric field self-correlation functions have been analyzed to obtain diffusion coefficients, D . The scattering particle diameters, d , have been evaluated by means of the Stokes-Einstein equation: $D = k_B T / 3\pi\eta d$ once provided the absolute temperature T , and the viscosity of the solution η . Owing to the low concentration of the systems, the latter can be assumed coincident with the one of the pure solvent, within the limits of experimental errors. The self-correlation function computed by using the Cumulant analysis [41], did not satisfactorily reproduce the experimental data, thus suggesting that the particles in suspension were polydisperse. Therefore, a more appropriate analysis was performed by means of the CONTIN method [42].

4.3. Synthesis of Ag-NPs

Ag-NP systems were prepared with a slight modification of reported procedure [14]: mother solutions of $[\text{Ag}(\text{NH}_3)_2]^+$ 15 mM and **AmCD** 6 mM were prepared in double-distilled water, previously degassed with a fine stream of Ar for 15 minutes. Then, samples were prepared by mixing in a dark vial the proper amounts of water, $[\text{Ag}(\text{NH}_3)_2]^+$ and **AmCD** solutions up to 14 mL. The samples, kept under Ar atmosphere, were placed in an oil bath thermostated at 40 °C, inoculated with 1 mL of formaldehyde solution 33.4 mM, and allowed to react for 90 minutes. UV-vis spectra of the samples were recorded immediately after the reaction time. **Catalysts I and II were carefully kept and stored in the dark before use. In order to collect a sample for FT-IR, 100 mL of Catalyst I were subjected to centrifugation at 5000 rpm for 15 minutes, and the resulting solid residue was isolated and lyophilized (yield 14.3 mg).**

4.4. Kinetics

Kinetic experiments were performed at 313 K, according to the following procedure. In a quartz cuvette the proper amount of a stock solution of catalyst (1.0 mM) was diluted in the proper amount of freshly double-distilled water (degassed with a fine stream of Ar for 15 minutes), in

such a way to have 2.65 mL of solution; then, 100 μL of a stock solution 3.0 mM of the substrate were added, and the mixture was thermostated. A 48.0 mM solution of NaBH_4 was prepared just before use by dissolving a weighed amount in a volumetric flask; then 250 μL were rapidly introduced in the cuvette, and the registration of the kinetic trace immediately started, following by UV-vis spectrophotometry the disappearance of the nitroarene substrate.

Acknowledgments

TEM micrographs were acquired at the *Centro Grandi Apparecchiature - UniNetLab - Università di Palermo* funded by *P.O.R. Sicilia 2000-2006, Misura 3.15 Quota Regionale*; Prof. Eugenio Caponetti and Dr. G. Nasillo are gratefully acknowledged for collaboration and useful discussion.

References and notes

- [1] G.W. Kabalka, R.S. Varma, "Reduction of Nitro and Nitroso compounds" in *Comprehensive Organic Synthesis*, Vol. 8, pag. 363-379, B.M. Trost and I. Fleming, Eds., Pergamon Press, Oxford (UK), 1991.
- [2] N. Pradhan, A. Pal, T. Pal, *Colloids Surf. A* 196 (2002) 247-257.
- [3] a) K. Esumi, K. Miyamoto, T. Yoshimura, *J. Colloid Interf. Sci.* 254 (2002) 402-405. b) K. Esumi, R. Isono, T. Yoshimura, *Langmuir* 20 (2004) 237-243. c) T. Endo, T. Yoshimura, K. Esumi, *J. Colloid Interf. Sci.* 286 (2005) 602-609.
- [4] a) K.P. Bankura, D. Maity, M.M.R. Mollick, D. Mondal, B. Bhowmick, M.K. Bain, A. Chakraborty, J. Sarkar, K. Acharya, D. Chattopadhyay, *Carbohydr. Polym.* 89 (2012) 1159–1165. b) G. Yang, Q. Lin, C. Wang, J. Li, J. Zhou, Y. Wang, C. Wang, *J. Nanosci. Nanotechnol.* 12 (2012) 3766-3774.
- [5] c) R. Eising, A.M. Signori, S. Fort, J.B. Domingos, *Langmuir* 27 (2011) 11860-11866.
- [6] L. Ai, J. Jang, *Biores. Technol.* 132 (2013) 374–377.
- [7] S. Pyne, S. Samanta, A. Misra, *Solid State Sci.* 26 (2013) 1-8.
- [8] S. Saha, A. Pal, S. Kundu, S. Basu, T. Pal, *Langmuir* 26 (2010) 2885-2893.

- [9] a) H. Ye, R.W.J. Scott, R.M. Crooks, *Langmuir*, 20 (2004) 2915-2920. b) J. Zheng, M. S. Stevenson, R.S. Hikida, P.G. Van Patten, *J. Phys. Chem. B* 106 (2002) 1252-1255.
- [10] K. Hayakawa, T. Yoshimura, K. Esumi, *Langmuir* 19 (2003) 5517-5521.
- [11] a) S. Pande, S.K. Ghosh, S. Praharaj, S. Painigrahi, S. Basu, S. Jana, A. Pal, T. Tsukuda, T. Pal, *J. Phys. Chem. C* 111 (2007) 10806-10813. b) Y. Huang, D. Li, J. Li, *Chem. Phys. Lett.* 389 (2004) 14-18. c) P.R. Gopalan, *Int. J. Nanosci.* 9 (2010) 487-494. d) P.F. Andrade, A. Fonseca de Faria, D. Soares da Silva, J. A. Bonacin, M.d.C. Gonçalves, *Colloid. Surf. B* 118 (2014) 289-297.
- [12] B.D. Loganathan, A.B. Mandal, *RSC Adv.* 3 (2013) 5238-5253.
- [13] a) J. Liu, S. Mendoza, E. Román, M.J. Lynn, R. Xu, A.E. Kaifer, *J. Am. Chem. Soc.* 121 (1999) 4304-4305. b) J. Liu, W. Ong, E. Román, M.J. Lynn, A.E. Kaifer, *Langmuir* 16 (2000) 3000-3002. c) J. Liu, W. Ong, A.E. Kaifer, C. Peinador, *Langmuir* 18 (2002) 5981-5983. d) Y. Guo, Y. Zhao, H. Wu, M. Fan, Y. Wei, S. Shuang, C. Dong, *J. Incl. Phenom. Macrocycl. Chem.* 78 (2014) 275-286. d) X. Li, Z. Qi, K. Liang, X. Bai, J. Xu, J. Liu, J. Shen, *Catal. Lett.* 124 (2008) 413-417.
- [14] P. Lo Meo, F. D'Anna, M. Gruttadauria, S. Riela, R. Noto, *Carbohydr. Res.* 347 (2012) 32-39.
- [15] It is worth stressing here that the synthesis of **AmCD** from native **β CD** requires two steps only, and therefore is much more straightforward and cheaper than the syntheses reported in literature of other polyaminocyclodextrin derivatives, obtained as pure individual products and mainly employed for polynucleotide complexation and gene transfection. See for instance: a) C. Ortiz Mellet, J.M. Benito, J.M. García Fernández, *Chem. Eur. J.* 16 (2010) 6728-6742. b) A. Méndez-Ardoi, M. Gómez-García, C. Ortiz Mellet, N. Sevillano, M.D. Girón, R. Salto, F. Santoyo-González, J.M. García Fernández, *Org. Biomol. Chem.* 7 (2009) 2681-2684. c) S. Srinivasachari, K.M. Fichter, T.M. Reineke, *J. Am. Chem. Soc.* 130 (2008) 4618-4627. d) J. Deng, N. Li, K. Mai, C. Yang, L. Yan, L.-M. Zhang, *J. Mater. Chem.* 21 (2011) 5273-5281.
- [16] A. Gangula, R. Podila, M. Ramakrishna, L. Karanam, C. Janardhana, A.M. Rao, *Langmuir* 27 (2011) 15268-15274.
- [17] J. Zeng, Q. Zhang, J. Chen, Y. Xia, *Nano Lett.* 10 (2010) 30-35.
- [18] N. Bingwa, R. Meijboom, *J. Mol. Catal. A* 396 (2015) 1-7.
- [19] a) P. Lo Meo, F. D'Anna, S. Riela, M. Gruttadauria, R. Noto, *Org. Biomol. Chem.* 1 (2003) 1584-1590. b) P. Lo Meo, F. D'Anna, S. Riela, M. Gruttadauria, R. Noto, *Tetrahedron* 63 (2007) 9163-9171.
- [20] P. Lo Meo, F. D'Anna, M. Gruttadauria, S. Riela, R. Noto, *Tetrahedron* 60 (2004) 9099-9111.

- [21] K.G. Thomas, "Surface Plasmon Resonances in Nanostructured Materials" in *Nanomaterials Chemistry*, pag. 185-218, C.N.R. Rao, A. Müller and A.K. Cheetham Eds., Wiley-VCH, Weinheim (Germany), 2007. It is worth stressing that polarity or refractive index variations may in turn be the outcome of a ligand exchange at the NP surface. For instance, it has been recently shown that the position of the SPR is significantly shifted in presence of halide ions. See: a) B.-H. Kim, J.-S. Lee, *Mater. Chem. Phys.* 149-150 (2015) 678-685. b) X.C. Jiang, A.B. Yu, *Langmuir* 24 (2008) 4300-4309.
- [22] a) Y. Zhu, M. Shen, Y. Xia, M. Lu, *Catal. Commun.* (2015) 64, 37-43. b) F. Valentini, D. Roscioli, M. Carbone, V. Conte, B. Floris, E.M. Bauer, E. Caponetti, D. Chillura-Martino, *Sens. Actuators B* 212 (2015) 248-255. c) M.L. Saladino, D. Chillura Martino, E. Kraveva, E. Caponetti *Catal. Commun.* 36 (2013) 10-15. d) E. Caponetti, L. Pedone, M.L. Saladino, D. Chillura Martino, G. Nasillo, *Microporous Mesoporous Mater.* 128 (2010) 101-107.
- [23] This estimation is based on the fact that the β CD torus alone is reported to have an average diameter of 1.54 nm (see ref. [20]), and that the length of a stretched diamine pendant chain can be estimated (MM2) as ca. 0.8 nm.
- [24] J. Szejtli, *Chem. Rev.* 98 (1998) 1743-1753.
- [25] S. Wunder, F. Polzer, Y. Lu, Y. Mei, M. Ballauff, *J. Phys. Chem. C* 114 (2010) 8814-8820.
- [26] Y. Gao, X. Ding, Z. Zheng, X. Cheng, Y. Peng, *Chem. Comm.* (2007) 3720-3722.
- [27] M. Blosi, S. Albionetti, S. Ortelli, A.L. Costa, M. Ortolani, L. Dondi, *New J. Chem.* 38 (2014) 1401-1409.
- [28] A.M. Signori, K. de O. Santos, R. Eising, B.L. Albuquerque, F. C. Giacomelli, J.B. Domingos, *Langmuir* 26(2010) 17772-17779.
- [29] K. Vasenth Kumar, K. Porkodi, F. Roche, *Catal. Comm.* 9 (2008) 82-84.
- [30] a) J.S. Zhang, W.N. Delgass, T.S. Fisher, J.P. Gore, *J. Power Sources* 164 (2007) 772-781. b) F. Lin, R. Doong, *Appl. Catal. A* 486 (2014) 32-41.
- [31] J. W. Rodriguez-Acosta, M. A. Mueses, F. Machuca-Martínez, *Int. J. Photoenergy* (2014) DOI: 10.1155/2014/817538.
- [32] G. Guella, B. Patton, A. Miotello *J. Phys. Chem C* 111 (2007) 18744-18750.
- [33] Q. Zhou, G. Qian, Y. Li, G. Zhao, Y. Chao, J. Zheng, *Thin Solid Films* 516 (2008) 953-956.
- [34] Of course, the fitting analysis is carried out directly on spectrophotometric data. For this purpose, equation (3) is trivially modified by posing: $C_0 = (Abs_0 - Abs_\infty) / \epsilon_{ArNO_2}$ and $|ArNO_2| = (Abs_t - Abs_\infty) / \epsilon_{ArNO_2}$; where Abs_0 and Abs_∞ are the initial and final absorbances respectively, Abs_t is the absorbance at a given time t, and ϵ_{ArNO_2} is the molar extinction coefficient of the substrate at the

operational wavelength. Noticeably, Abs_{∞} keeps into account the possible contribution to the overall absorbance from the Ag-NP catalyst (the contribution from the aniline product is negligible).

[35] a) S. Jana, S.K. Gosh, S. Nath, S. Pande, S. Paharaj, S. Panigrahi, S. Basu, T. Endo, T. Pal, *Appl. Catal. A* 313 (2006) 41-48. b) K.B. Narayanan, N. Sakthivel, *Biores. Technol.* 102 (2011) 10737-10740.

[36] The latter statement needs to be briefly justified. As a matter of fact, it has to be reminded that most of the **AmCD** units present in the system cannot interact with the NPs surface and are delivered into solution, as discussed previously. Delivered **AmCD** can form host-guest inclusion complexes with the nitroarene substrate. The molar fraction of units engaged in this process depends, in turn, on the binding constant K_{CD} and on the analytical concentration of the substrate, and it can be calculated algebraically. Now, by assuming that the K_{CD} values for nitroarenes **1-8** towards **AmCD** are similar to those found in the case of native **β CD** (see ref. [18] and [19]), it follows that the concentration of a possible ($ArNO_2 \cdot AmCD$) inclusion complex is actually negligible with respect to free **AmCD**.

[37] X. Li, J. Wang, Y. Zhang, M. Li, J. Liu, *Eur. J. Org. Chem.* (2010) 1806-1812.

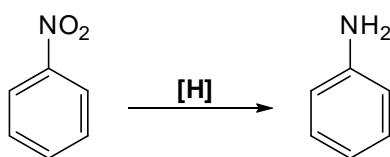
[38] a) T.-X. Lü, D.-B. Zhang, S.-J. Dong, *J. Chem. Soc., Faraday Trans.* 85 (1989) 1439-1445. b) H.-J. Schneider, F. Hackett, V. Rüdiger, H. Ikeda, *Chem. Rev.* 98 (1998) 1755-1785. c) G.M. Bonora, R. Fornasier, P. Scrimin, U. Tonellato, *J. Chem. Soc., Perkin Trans.* 2 (1985) 367-369. d) O.S. Tee, C. Mazza, X.-X. Du, *J. Org. Chem.* 55 (1990) 3603-3609. e) P. Lo Meo, F. D'Anna, S. Riela, M. Gruttadauria, R. Noto, *Tetrahedron* 58 (2002) 6039-6045. f) P. Lo Meo, F. D'Anna, S. Riela, M. Gruttadauria, R. Noto, *Tetrahedron* 65 (2009) 2037-2042. g) P. Lo Meo, F. D'Anna, M. Gruttadauria, S. Riela, R. Noto, *Tetrahedron* 65 (2009) 10413-10417.

[39] F. D'Anna, P. Lo Meo, S. Riela, M. Gruttadauria, R. Noto, *Tetrahedron* 57 (2001) 6823-6827.

[40] It is worth noting that in our particular system, unfortunately, it is very hard to verify otherwise the occurrence of radical-involving mechanistic pathways. As a matter of fact, classical radical scavengers such as phenols or thiols cannot be employed because, being acidic species, they immediately decompose the BH_4^- ion.

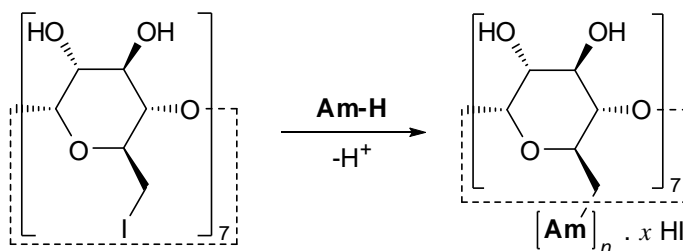
[41] D. E. J. Koppel, *Chem. Phys.* 57 (1972) 4814-4820

[42] a) S.W. Provencher, *Macromol. Chem.* 180 (1979) 201-209. b) S.W. Provencher, *Comput. Phys. Commun.* 27 (1982) 213-227.

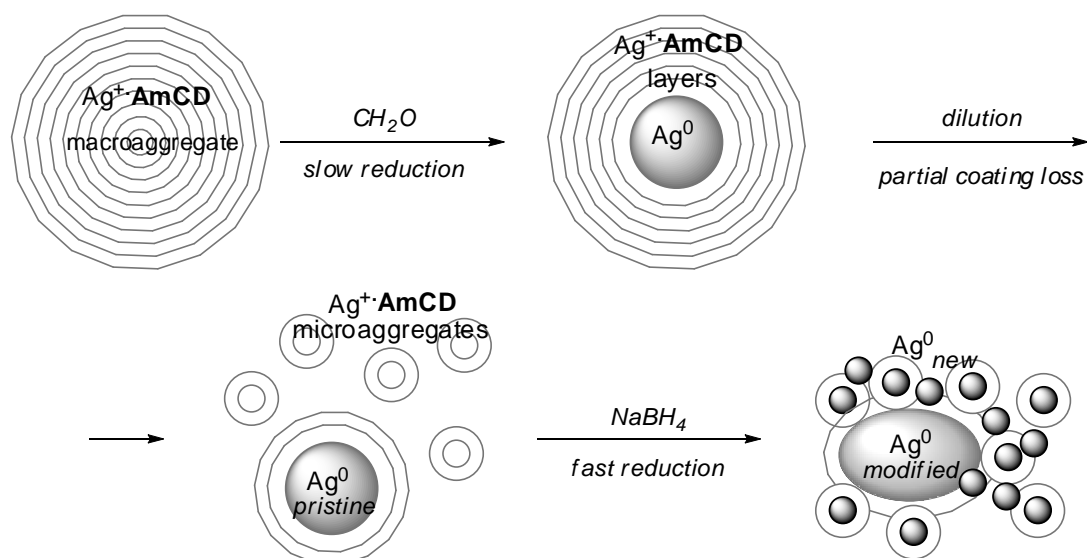


[H] = LiAlH₄ or Fe/HCl or H₂/Pd

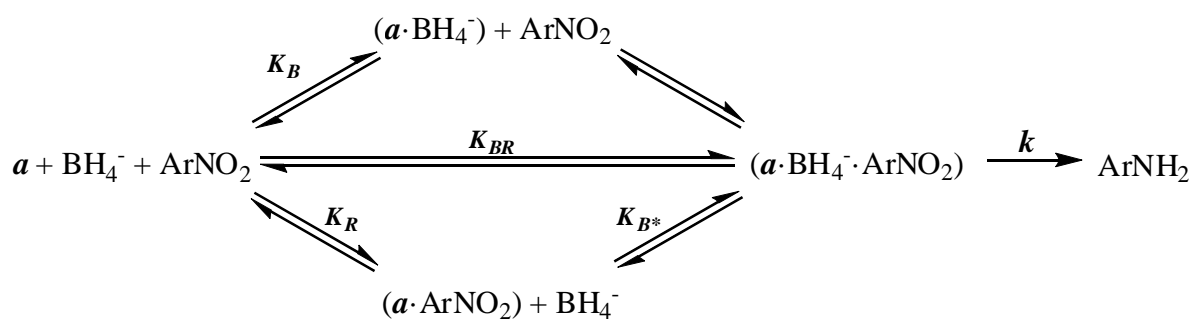
Scheme 1



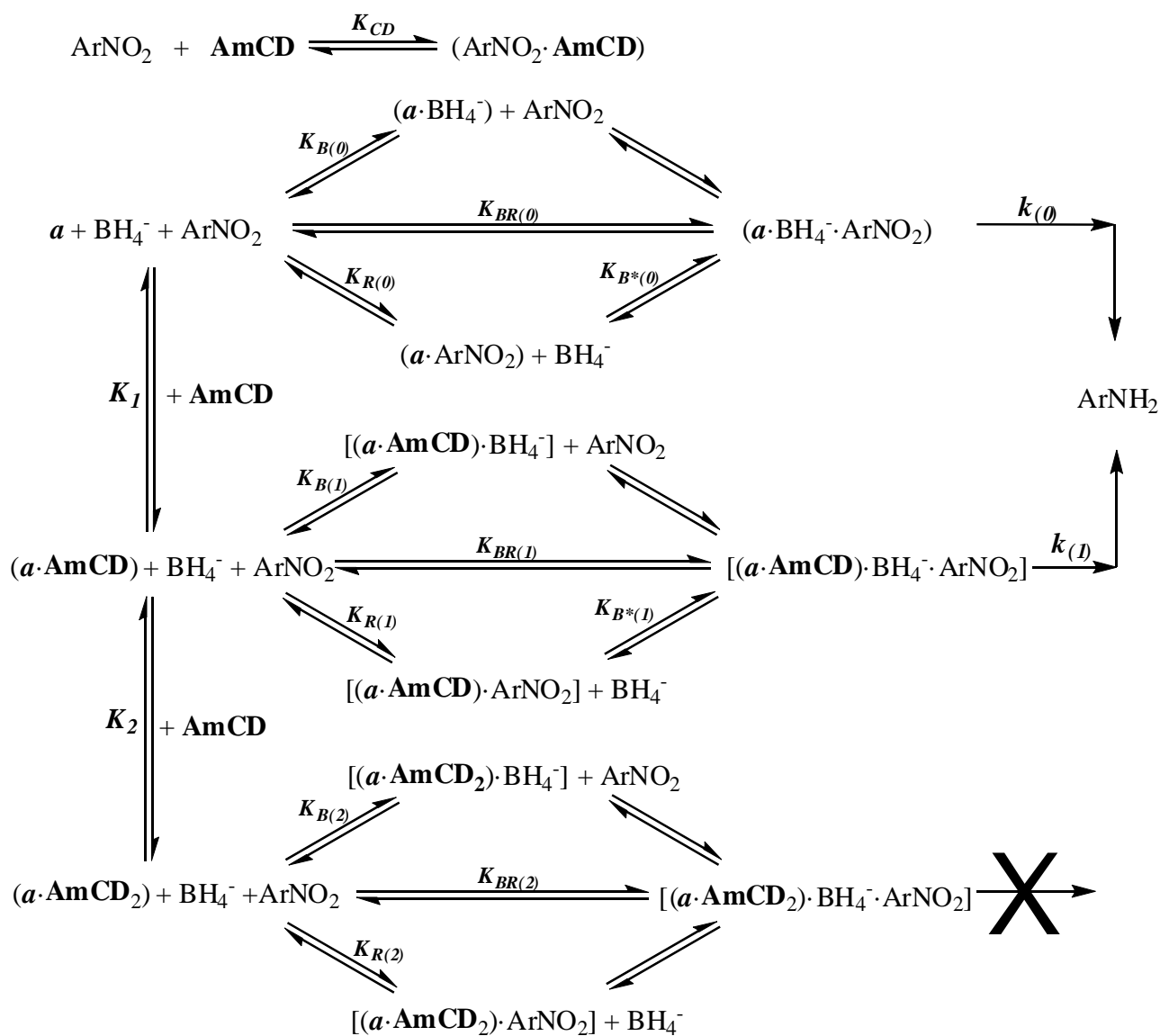
Scheme 2



Scheme 3



Scheme 4



Scheme 5

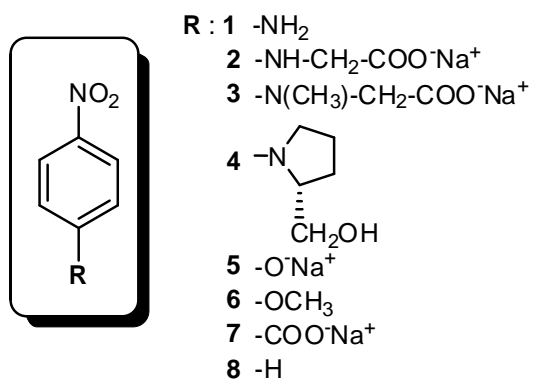


Figure 1. Nitroarene substrates

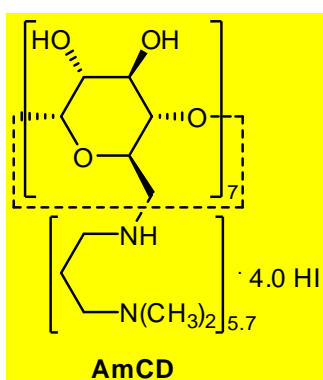


Figure 2. Structure of AmCD

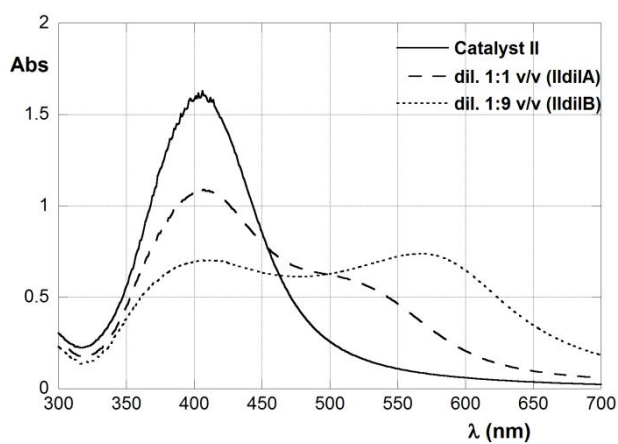


Figure 3. Normalized UV-vis spectra for pristine Catalyst II and its dilutions

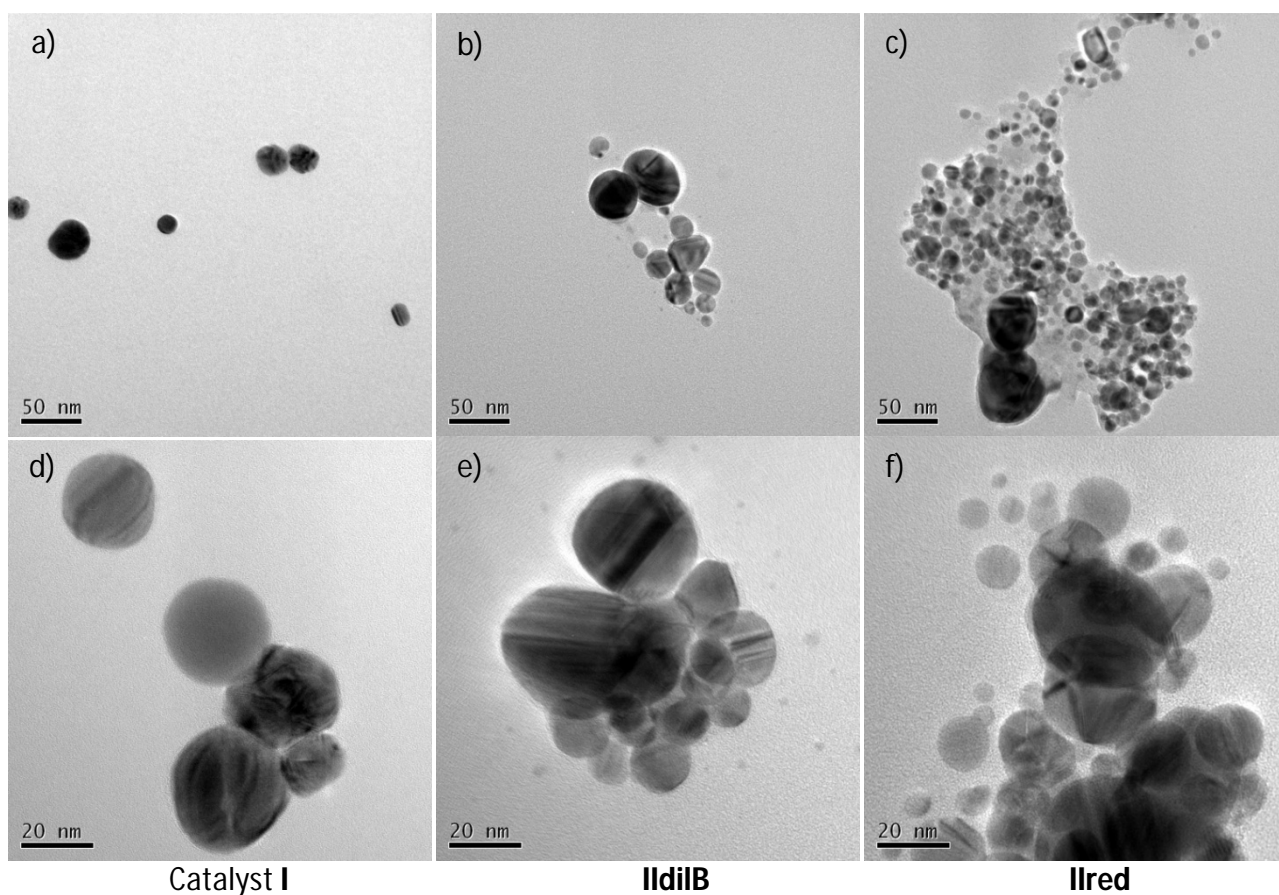


Figure 4. TEM micrographs of Catalyst I (a,d), IldiB (b,e) and Ired (c,f). Micrographs a, b and c acquired at a 50000X magnification; micrographs d, e and f acquired at a 150000X magnification.

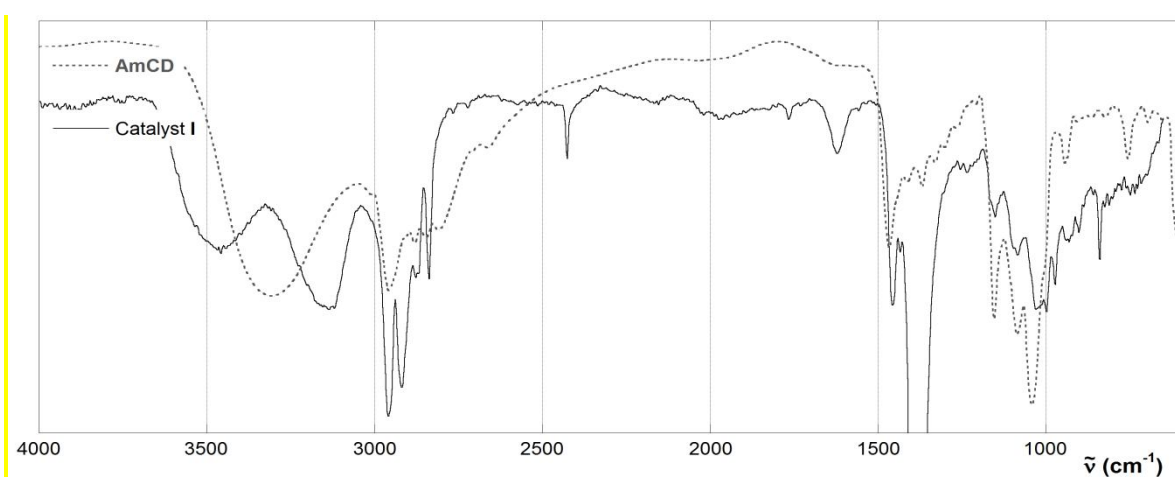


Figure 5. FT-IR spectra of AmCD (---) and Ag NPs precipitate from Catalyst I (—).

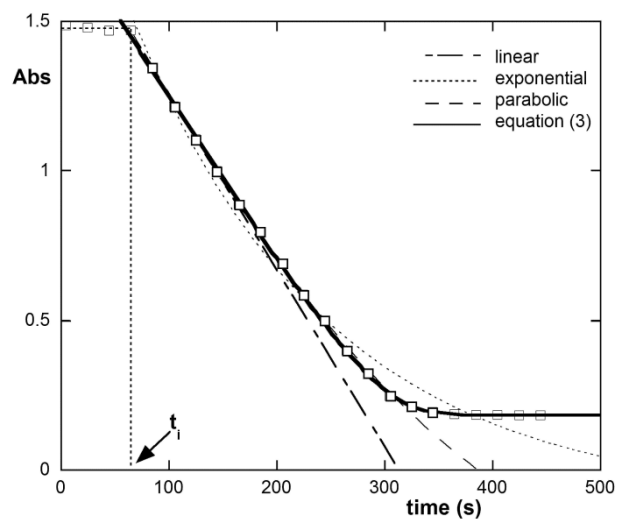


Figure 6. Kinetic trace (squares) for the reaction of **1** (0.1 mM) with NaBH_4 (4.0 mM) in the presence of catalyst **II** (50 μM).

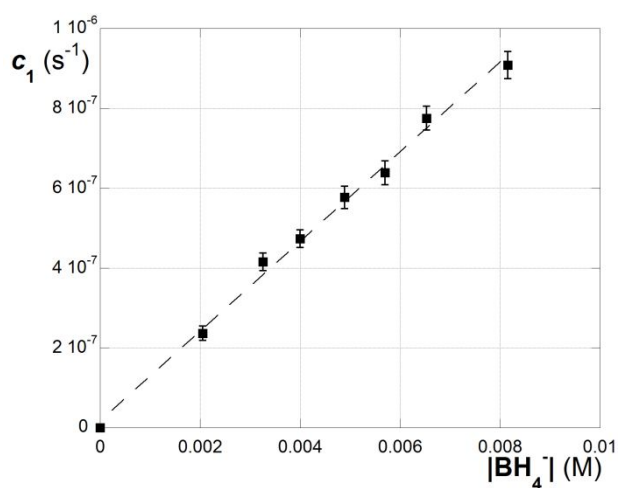


Figure 7. Dependence of the initial reaction rate (c_1) vs. BH_4^- concentration for the reaction of **1** (0.1 mM) in the presence of catalyst **II** (50 μM).

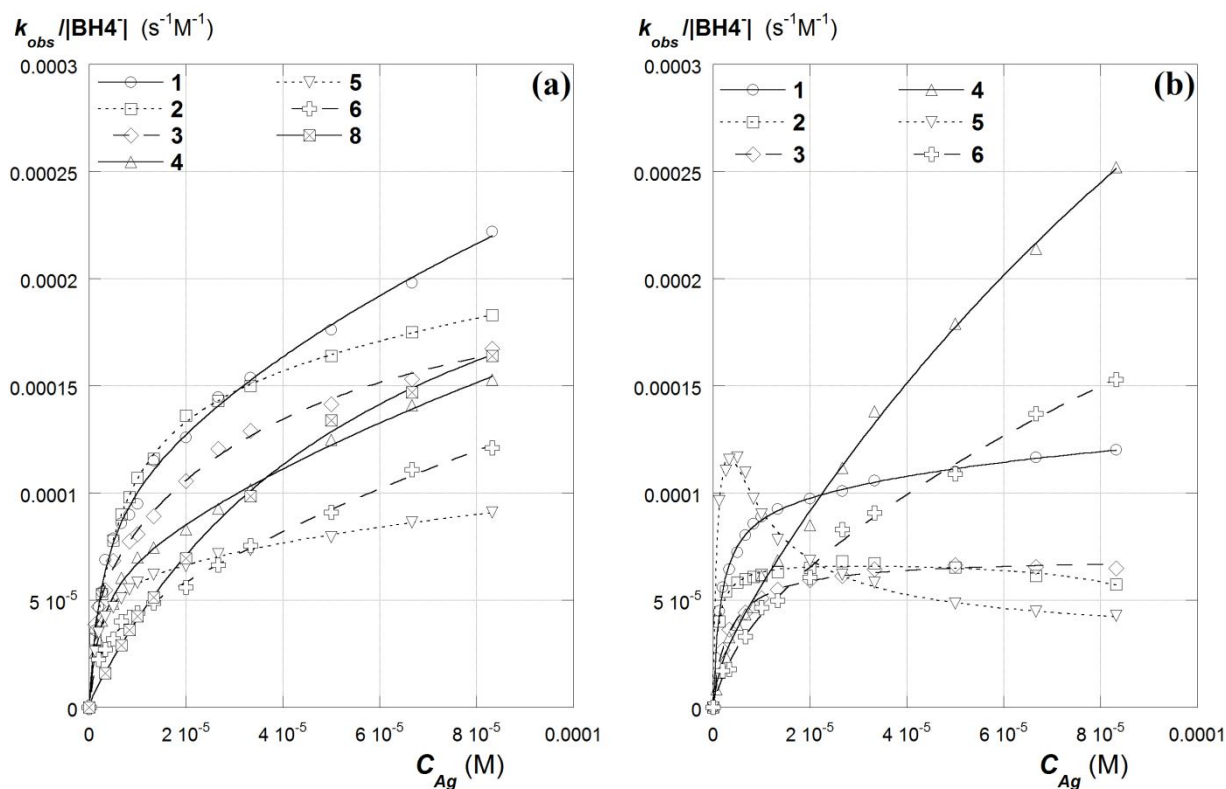


Figure 8. Dependence of $k_{obs}/[BH_4^-]$ on C_{Ag} for Catalyst I (a) and Catalyst II (b).

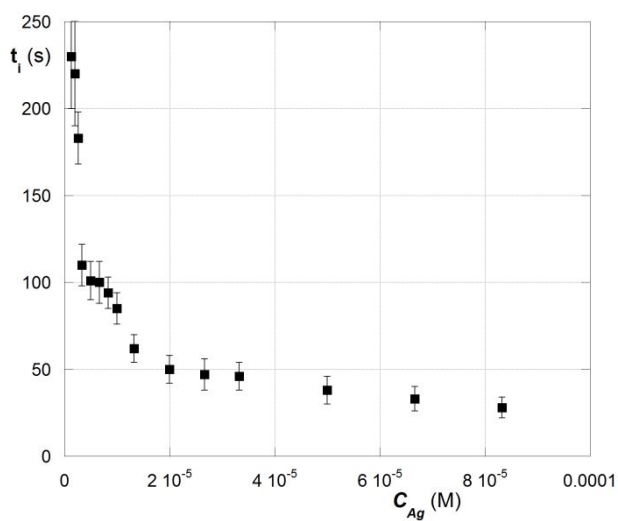


Figure 9. Induction times t_i for the reaction of 1 with Catalyst I at different concentrations.

Table 1. ε values for the AmCD/Ag NP systems at the relevant λ_{max} .

| | | Ag ⁺ (mM) | | | | |
|---------------|------|------------------------|-------------|-------------|------|--------|
| | | 0.2 | 0.5 | 1.0 | 2.0 | 5.0 |
| AmCD (mN) | 0.4 | No reaction | n.d. | 12420 | n.d. | n.d. |
| | 1.0 | n.d. | 4670 | 10020 | n.d. | n.d. |
| | 2.0 | No reaction | No reaction | 5540 | 9240 | Turbid |
| | 4.0 | n.d. | n.d. | 440 | 5060 | n.d. |
| | 10.0 | n.d. | n.d. | No reaction | n.d. | Turbid |

Table 2. Values of $k_{obs,0}$, $k_{obs,1}$, $K_{app,1}$ and $K_{app,2}$.

| Sub. | catalyst I | | | | | catalyst II | | | | |
|------|------------|---|---|--|--|-------------|---|---|--|--|
| | eq. | $k_{obs,0}$ (s ⁻¹ M ⁻¹) | $k_{obs,1}$ (s ⁻¹ M ⁻¹) | $K_{app,1}$ (10 ⁻⁶ M ⁻¹) | $K_{app,2}$ (10 ⁻⁶ M ⁻¹) | eq. | $k_{obs,0}$ (s ⁻¹ M ⁻¹) | $k_{obs,1}$ (s ⁻¹ M ⁻¹) | $K_{app,1}$ (10 ⁻⁶ M ⁻¹) | $K_{app,2}$ (10 ⁻⁶ M ⁻¹) |
| 1 | (11) | 36.2±1.4 | 1.30±0.07 | 8.4±0.8 | n.d. | (10) | 62±3 | 2.0±1.0 | 3.9±0.4 | 0.8±0.4 |
| 2 | (11) | 29.0±0.4 | 0.40±0.03 | 5.1±0.2 | n.d. | (10) | 65±2 | (< 0.2) | 5.2±0.2 | (<0.4) |
| 3 | (11) | 36.0±2.0 | 0.88±0.09 | 10.0±1.8 | n.d. | (10) | 23±2 | 0.6±0.4 | 2.0±0.2 | 0.5±0.3 |
| 4 | (11) | 26.7±1.1 | 1.00±0.05 | 9.8±1.2 | n.d. | (11) | 11±2 | 2.4±0.1 | 0.8±0.2 | n.d. |
| 5 | (11) | 32.0±0.6 | 0.33±0.02 | 13.7±0.7 | n.d. | (10) | 131±2 | 6.3±2.0 | 3.2±0.8 | 1.2±0.3 |
| 6 | (11) | 16.9±0.7 | 0.93±0.03 | 10.0±1.2 | n.d. | (11) | 7±1 | 1.1±0.1 | 0.44±0.1 | n.d. |
| 7 | - | n.d. | n.d. | n.d. | n.d. | - | n.d. | n.d. | n.d. | n.d. |
| 8 | (11) | 5.2±0.3 | 0.67±0.07 | 0.84±0.07 | n.d. | - | n.d. | n.d. | n.d. | n.d. |